Current Topics in Biophysics 2005, 29(1-2), 139-156

MECHANISM OF FORMATION OF EPR-ACTIVE MONONITROSYL-IRON COMPLEXES WITH DITHIOCARBAMATES IN BIOSYSTEMS

ANATOLY F. VANIN[1,2], ALEXANDER P. POLTORAKOV[1], VASAK D. MIKOYAN[1], LIOUDMILA N. KUBRINA[1], ERNST VAN FAASSEN[2].

[1]Semenov Institute of Chemical Physics, Russian Academy of Sciences, Moscow, Russia;
[2]Interface Physics, Debye Institute, Utrecht University, The Netherlands

The in-vivo mechanism of NO trapping by iron-dithiocarabamate complexes is revised. Contrary to common belief, we find that in biological systems the NO radicals are predominantly trapped by ferric iron-dithiocarbamates. Therefore, the trapping leads to diamagnetic mononitrosyl complexes which cannot be directly detected with Electron Paramagnetic Resonance spectroscopy. The diamagnetic mononitrosyl complexes are far easier reduced with L-cysteine, glutathione or ascorbate to ferrous state than their non-nitrosyl counterpart. The reduction could also proceed through the mechanism of reductive nitrosylation that could be accompanied with the accumulation of EPR-silent S-nitrosylated dithiocarbamate molecules. The latter as well as diamagnetic mononitrosyl iron complexes with dithiocarbamate compose the majority of the compounds in biological systems containing trapped NO molecules as compared with the amount of EPR-detectable paramagnetic mononitrosyl iron complexes with dithiocarbamates. The exogenous reductant, dithionite being added to tissue preparations ex-vivo initiated sharp increase in the amount of paramagnetic mononitrosyl iron complexes with dithiocarbamates. This treatment led to significantly higher yields from NO trapping experiments on mice. Concomitant background signal from copper-dithiocarbamate complexes was eliminated, thereby facilitating the quantification of yields from NO trapping.

INTRODUCTION

Iron-dithiocarbamate complexes are now widely used as selective traps to detect and quantitate nitric oxide (NO) in solutions, cultured cells, or mammalian and plant tissues (Vanin, Mordvintcev & Kleschyov, 1984; .Lai & Komarov, 1994; Vanin, 1999: Vanin, Huisman & van Faassen, 2002; Vanin, Svistunenko, Mikoyan, Serezhenkov, Fryer, Baker & Cooper, 2004). The conventional viewpoint assumes that NO radical be trapped by the diamagnetic ferrous Fe^{2+}-dithiocarbamate complexes. The resulting adduct is a paramagnetic mononitrosyl-iron complex (MNIC) that may be detected by electron paramagnetic resonance (EPR) spectroscopy. This conventional viewpoint is incompatible with the presence of considerable amounts of molecular oxygen in any biological material. Given the high rate of the oxidation of Fe^{2+}-dithiocarbamates with oxygen (the rate constant $k = 5\times10^5\ M^{-1}s^{-1}$, Tsuchiya, Jiang, Yoshizumi, Tamaki, Houchi, Minakuchi, Fukuzawa & Mason, 1999), the presence of oxygen will rapidly oxidize the available iron complexes to ferric state. Indirect evidence for this complete oxidation comes from the experimental observation that yields of paramagnetic MNIC in animal tissues do not depend on whether the iron be suppleted in ferrous or ferric form (Mikoyan, Kubrina, Serezhenkov, Stukan & Vanin, 1997). The redox state of the traps and MNIC adducts is ultimately determined by the properties of the biological sample itself.

In this paper we address two questions: First, the redox state of the iron complex which traps the NO radical. Second, the redox pathways which bring the mononitrosyl complexes to reduced paramagnetic state.

The Scheme 1 illustrates that two pathways exists as potential candidates for the transformation of oxidized traps (complex (I) to paramagnetic adducts (complex (IV)): (i) The counterclockwise

$$\begin{array}{ccc} Fe^{3+}\text{-DTC (I)} & \xrightarrow{NO} & NO\text{-}Fe^{3+}\text{-DTC (III)} \\ \Updownarrow & & \Updownarrow \\ Fe^{2+}\text{-DTC (II)} & \xrightarrow{NO} & NO\text{-}Fe^{2+}\text{-DTC (IV)} \end{array}$$

Scheme 1: The four possible iron-dithiocarbamate (Fe-DTC) complexes considered in this paper. The oxidized mononitrosyl-iron complex (III) is diamagnetic, whereas the reduced (IV) complex is paramagnetic (S=1/2). The conventional viewpoint of NO trapping is the direct transformation of complex (II) into (IV) by inclusion of a nitrosyl ligand.

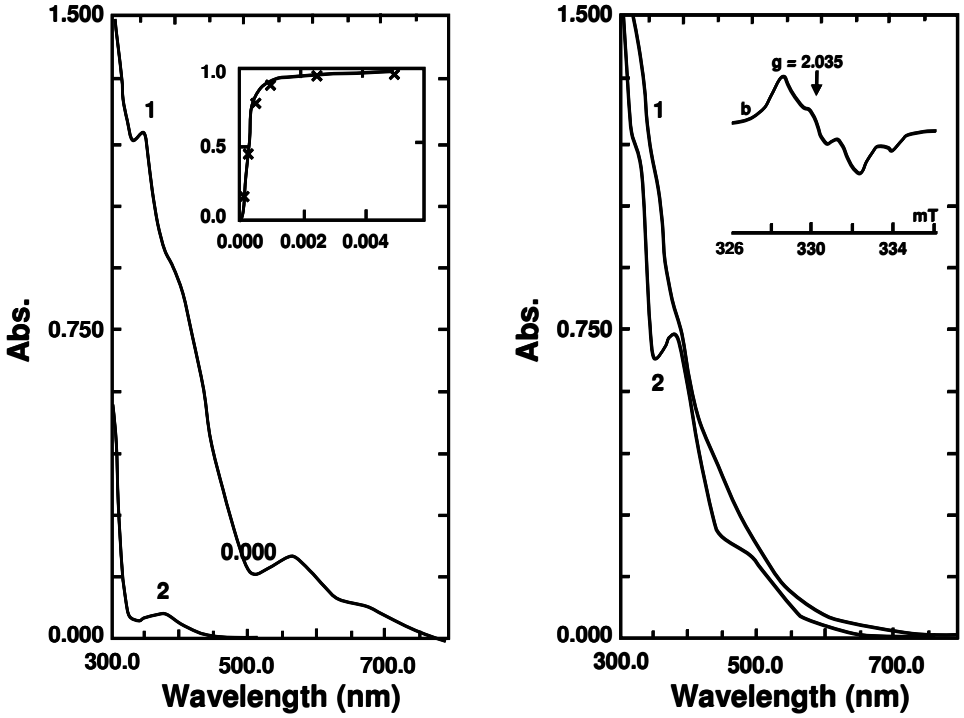

Fig.1 Optical adsorption spectra of Fe-MGD complexes (left panel) and their nitroso adducts (right panel) in 150 mM Hepes buffer solutions, pH 7.4. Left panel : spectra 1 and 2 are the absorption of $Fe^{3+}(MGD)_2$ and $Fe^{2+}(MGD)_2$ complexes respectively. The dependence of $Fe^{3+}(MGD)_2$ complex amounts from MGD concentrations monitored with the absorption at 340 nm is shown in inset. Right panel : spectra 1 and 2 are the absorption of NO-$Fe^{3+}(MGD)_2$ and NO-$Fe^{2+}(MGD)_2$ complexes, respectively. The EPR spectrum of NO-$Fe^{2+}(MGD)_2$ complex recorded at 77K is shown in inset.

path, where complex (I) is first reduced by some endogenous reductant, and the intermediate complex (II) be subsequently nitrosylated by the trapping of an NO radical. This first pathway is compatible with the conventional viewpoint; (ii) The second pathway runs clockwise: As a first step, complex (I) is nitrosylated and the ensuing diamagnetic complex (III) be subsequently reduced by an endogenous reducers to the paramagnetic NO-Fe^{2+}-dithiocarbamate adduct complex (IV). This second pathway is at odds with the conventional viewpoint.

In principle, both pathways are possible, since the redox reactions (I) $\leftrightarrow$ (II) and (III) $\leftrightarrow$ (IV) are both reversible. The redox properties of the system under consideration decide which reaction channel will dominate. Evidently, the pathway with higher kinetics constants will dominate. We have used optical and EPR spectroscopy to study the nitrosylation and reduction reactions of Fe-DTC complexes and their nitroso-adducts. In view of its widespread application, we chose N-methyl-D-glucamine dithiocarbamate (MGD) ligands which form hydrophilic Fe-DTC complexes. In this paper we present evidence that the clockwise pathway be dominant in biological systems. The insight in the mechanism of adduct formation allows us to enhance the yield of nitrosyl adducts from biological samples.

MATERIALS AND METHODS

Materials

The following reagents were used: sodium DETC, L-cysteine, sodium ascorbate, reduced glutathione, sodium dithionite, HEPES and lipopolysaccharide from Esherichia coli (serotype 005:b5) were purchased from Sigma. Ferrous sulfate was from Fluka. N-methyl-D-glucamine dithiocarbamate (MGD) was synthesized according to the recipe described in (Shinobu, Jones & Jones, 1984). S-nitrosocysteine (cys-NO) or S-nitrosoglutathione (GS-NO) were synthesized as described elsewhere (Vanin, Muller, Alencar, Lobysheva, Nepveu & Stoclet, 2002). Gaseous NO was obtained by the reaction of $FeSO_4$ and $NaNO_2$ in 0.1 M HCl and then purified by the method of low-temperature sublimation in an evacuated system.

Optical and EPR assays

The shape and temporal kinetics of optical spectra of iron-MGD complexes and their nitroso ad-

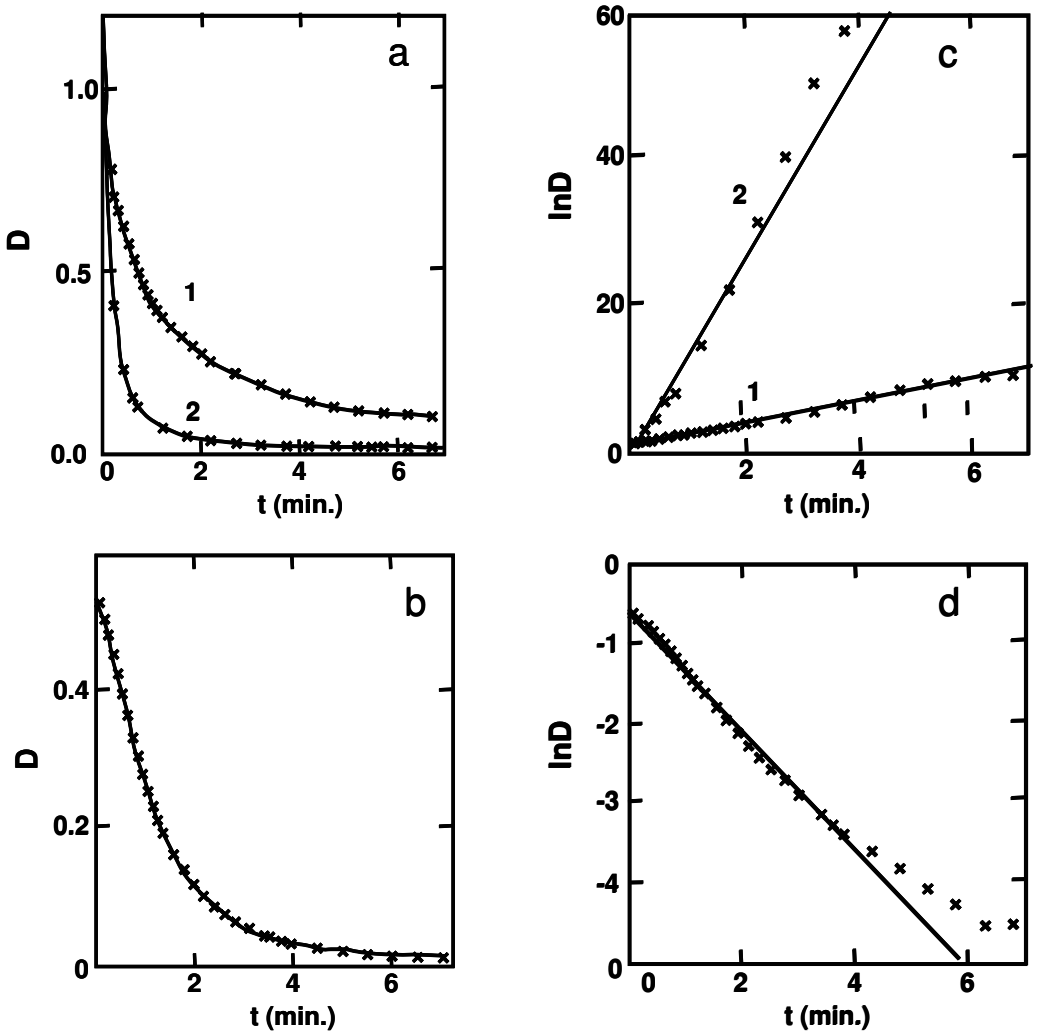

Fig. 2. The kinetics curves of the reactions between 0.1 mM $Fe^{3+}(MGD)_2$ complex and L- cysteine (a,c) or glutathione (b,e) in 150 mM Hepes buffer solutions, pH 7.4. L-cysteine or glutathione were added to the solutions at the amounts of 1 and 5 mM (a, c; curves 1 and 2) or 5 mM (b,d) respectively. The process of bleaching of the solutions was monitored with the absorption at 385 nm. Crossed curves are experimental ones; solid curves are correspondent to the reactions followed with second or first order rate low rate in $Fe^{3+}(MGD)_2$ complex (a,c) or (b,d), respectively. The reactions proceeded at ambient temperature.

adducts were recorded at ambient temperature in 150 mM Hepes buffer (pH 7.4) using UV-2501PC (Shimadzu Europa GmbH, Duisburg, Germany) or Varian Cary 300 Bio spectrometers(Varian, USA) in a 3-ml open cuvettes with 10 mm optical pathway.

The shape and temporal kinetics of EPR spectra were recorded at 77 K. Samples consisted of frozen 200 μl aliquots drawn by syringe from reaction mixtures and snap frozen in liquid nitrogen. The aliquots were placed in the center of a ER4103TM cavity (Bruker, Karlsruhe, Germany) equipped with a liquid finger quartz dewar filled with liquid nitrogen. Microphonics due to evaporation of the nitrogen was minimized by cotton stoppers just below and above the sample. The EPR spectra were recorded on a modified X-band EPR radiospectrometer ESP 300 (Bruker, Karlsruhe, Germany) at a modulating frequency of 100 kHz, modulation amplitude 0.5 mT, microwave power 10 mW, and microwave frequency near 9.5 GHz. Spin densities were estimated by comparing the doubly integrated intensity with those from reference solutions containing known concentrations of MNIC-MGD complexes.

Experiments on mice

White male mice of BULB line weighing 18-20 g were also used in experiments. Bacterial LPS added intraperitonealy to animals at the dose of 2 mg/kg stimulated the formation NO in various organs during a period of 4 hours after its administration to the animals. To detect NO,

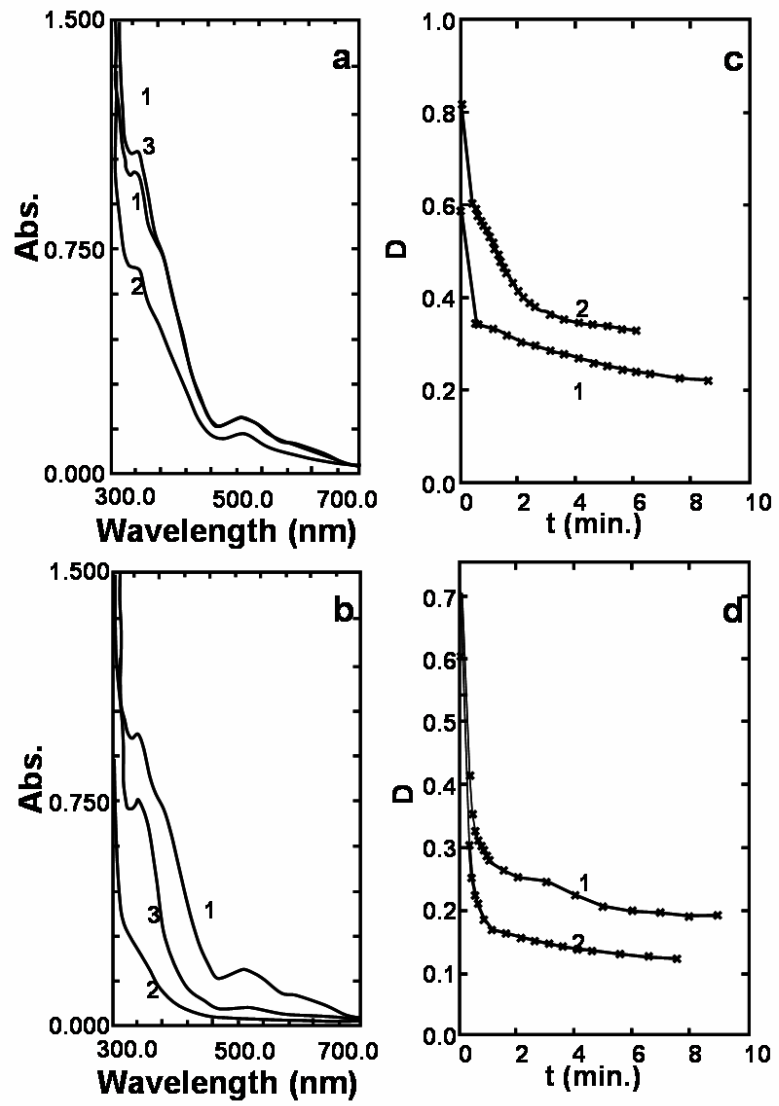

Fig.3. The optical and kinetics characterizations of the reactions between 0.1 mM $Fe^{3+}(MGD)_2$ complex and Na-ascorbate (a,c) or Na-citrate (b,d) in 150 mM Hepes buffer solutions, pH 7.4. Panel a: optical absorption of the solutions 0.1 mM Fe^{3+}+ 1 mM MGD, 0.1 mM Fe^{3+}+ 1 mM MGD + 1 mM ascorbate or 0.1 mM Fe^{3+}+ 2 mM MGD + 1 mM ascorbate (curves 1, 2 or 3, respectively); Panel b: optical absorption of the solutions 0.1 mM Fe^{3+}+ 1 mM MGD, 0.1 mM Fe^{3+}+ 1 mM MGD + 0. 1 mM citrate or 0.1 mM Fe^{3+}+ 10 mM MGD + 1 mM citrate (curves 1, 2 or 3, respectively); Panel c: kinetics curves of bleaching of the 0.1 mM $Fe^{3+}(MGD)_2$ solutions at action of 1mM or 5 mM ascorbate (curves 1 or 2, respectively). Panel d: kinetics curves of bleaching of the 0.1 mM $Fe^{3+}(MGD)_2$ solutions at action of 0.1mM or 0. 5 mM citrate (curves 1 or 2, respectively). Kinetics of bleaching was monitored with the absorption at 385 nm.

ministration to the animals. To detect NO, DETC and Fe^{2+}-citrate were injected into mice intraperitoneally or subcutaneously, respectively in 0.2 ml of 15 mM Hepes buffer (pH 7.4) in the doses: DETC, 500 mg/kg; FeSO4, 37.5 mg/kg; sodium citrate, 187.5 mg/kg. These compounds were injected 10 or 30 min before sacrifice of the animal by decapitation. The animals were anesthesized with ketamin just prior to decapitation. The various tissues were freshly extracted, cleaned by rinsing with water and snap frozen in liquid nitrogen for EPR assay. Subsequent reduction of the tissue samples with dithionite was performed by thawing, immersed in 150 mM Hepes buffer, pH 7.4 (1 ml per 1 g of tissue) and suppletion of 10 mM dithionite. After 30 min. incubation the samples were refrozen in liquid nitrogen for EPR measurements.

Data evaluation

All assays were done in duplicate and were repeated at least three times. The yields of paramagnetic complex IV are presented as means ± s.e.m.

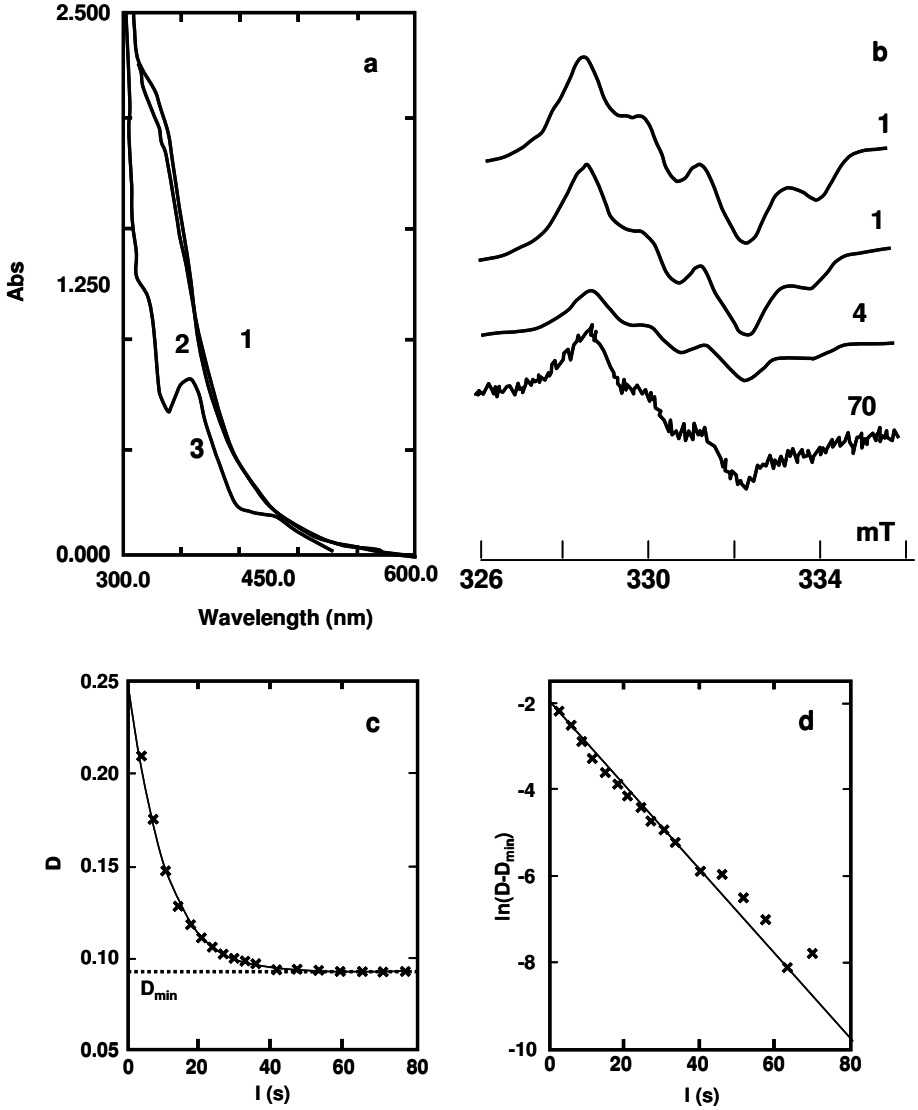

Fig.4. The optical (a), EPR (b) and kinetics chatacteristics (c,d) of stable NO-$Fe^{3+}(MGD)_2$ complex in deoxygenated 150 mM Hepes buffer solutions, pH 7.4 in the presence of 1 mM MGD. Panel a: optical absorption spectra of 0.1 mM $Fe^{3+}(MGD)_2$ solutions 1 or 10 min. after addition of 1.2 mM cys-NO (curves 1 or 2, respectively) resulting in the formation of stable NO- $Fe^{3+}(MGD)_2$ complex. Curve 3 is the spectrum of the solutions of stable NO- $Fe^{3+}(MGD)_2$ complex after addition of 5 mM ascorbate. Panel b: (a) EPR spectra from the solution of stable NO-$Fe^{3+}(MGD)_2$ complex, (b) from prepation (a) after addition of 5 mM MGD; (c) from preparation (a) after addition of 5 mM ascorbate; (d) from the solution of 0,1 mM paramagnetic NO-$Fe^{2+}(MGD)_2$ complex. The amplifications of the EPR spectrometer in arbitrary units are shown at right side. Recordings were made at 77 K. Panels c,d: The kinetics curves of the reaction of the formation of stable NO- $Fe^{3+}(MGD)_2$ complex. Crossed curves are experimental ones; solid curves are correspondent to the reactions followed with second order rate low in $Fe^{3+}(MGD)_2$ complex. The reaction proceeded at ambient temperature. Kinetics was monitored with the absorption at 514 nm.

RESULTS

Optical and EPR characteristics of iron-MGD complexes and their nitroso adducts.

As reported before (Vanin, Liu, Samouilov, Stukan & Zweier, 2000), aqueous solutions of the Fe^{3+}-MGD complexes are orange brown in color exhibiting three absorption bands at 340, 385 and 514 nm. Similar absorption was observed in our experiments for the solutions of Fe^{2+}-MGD complexes oxidized to Fe^{3+} state by shaking solutions in air (Fig. 1, left panel). However the extinction coefficients of these bands (14 000, 10 200 and 2 400 $M^{-1}cm^{-1}$, respectively) proved to be less than those estimated in (Vanin *et al*, 2000). The reason of the difference remains obscure. The dependence

of Fe^{3+}-MGD complex amounts from MGD concentrations in the solution at 0.1 mM concentration of iron is shown in Fig.1, left panel, inset. Taking into account the chemical equilibrium between of Fe^{3+}-$(MGD)_n$ complex and its constituents (Fe^{3+} + nMGD $\leftrightarrow$ $Fe^{3+}(MGD)_n$) the conventional analysis of this concentration curve (see Appendix) led to the value of n equal to 2. Phrased otherwise, even for excess MGD concentrations up to 5 mM, the Fe^{3+}-MGD complex includes 2 MGD ligands. It is reasonable to suggest that including hydroxyl ion to the complex ensures the neutralization of positive charge of the complex. As to including third MGD ligand to the complex the bulk size of the molecule could interfere this binding.

In accordance with previous data (Vanin *et al*., 2000) frozen Fe^{3+}-MGD solutions in 150 mM Hepes buffer (pH = 7.4) have an EPR absorption near $g = 4.3$ which is characteristic of a high spin Fe^{3+} complex (S = 5/2). This EPR absorption is lost upon addition of the strong reductant dithionite (data not shown). The resulting reduced Fe^{2+}-MGD complexes were colorless. Significantly, the EPR signal from high spin Fe^{3+} is also lost from buffered Fe^{3+}-MGD solutions upon a few minutes of bubbling with purified NO gas (data not shown). In this case, the color of the solutions changed from initial orange-brown to final yellow. The yellow spectrum characteristic of NO-Fe^{3+}-MGD complex (complex III) did not show prominent absorption bands in the visible region, except for a poorly resolved band at 314 nm (Fig. 1, right panel). Subsequent addition of dithionite or ascorbate to the solution changed its color to green. This solution showed three absorption bands at 314, 365 and 450 nm with the extinction coefficients of 12700, 6750 and 1700 sm^{-1}, respectively (Fig. 1, right panel). The shape of the optical absorption spectrum was identical to that obtained with NO treatment of Fe^{2+}-MGD complex. In addition, the green solution gave an intensive EPR signal at $g = 2.035$ (Fig. 1, right panel, inset) with the characteristic hyperfine triplet structure known from from NO- Fe^{2+}-MGD complex IV(Vanin *et al*., 2000).

Reduction of Fe^{3+}-MGD complexes (complex I) with L-cysteine or glutathione anions.

The reduction of ferric MGD complexes was investigated in buffered solution (150 mM Hepes, pH 7.4) which had been deoxygenated by bubbling with argon. We considered mainly L-cysteine and reduced glutathione , since all are known as important endogenous biological reductants (Halliwell & Gutteridge, 1999). The reduction of ferric to ferrous complexes (I) $\rightarrow$ (II) is visible to the naked eye as a bleaching of the solutions. Fig. 2 (left panels) shows the kinetics of bleaching by cysteine or glutathione in anionic form. Subsequent shaking the solutions in air restores the original color within a few seconds (data not shown).

The kinetics of the reduction reactions was followed spectrophotometrically under conditions of high as well as low ratios of iron vs. reductant. i.e. 1-5 mM of reductant versus 0.1 mM of the complex or 0.5 mM of the complex versus 0.05 mM of reductant, respectively. Fig. 2 shows the data with excess reductant. With cysteine (Fig. 2.a, c) the kinetics become linear when plotted as $1/D$, suggesting second order dependence in $Fe^{3+}(MGD)_2$. At high iron/cysteine ratios this reaction is seen to be second order in cysteine as well (data not shown), and suggest the reduction mechanism as:

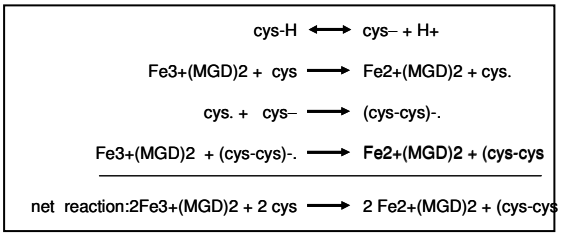

Scheme 2

Interestingly, the kinetics for glutathione is different: Under excess glutathione the kinetics become linear when plotted as ln D (Fig. 2 b,d) suggesting a reaction first order in $Fe^{3+}(MGD)_2$ complexes. At high iron/glutathione ratios the reaction is observed to be first order in glutathione as well (data not shown) and suggest a reduction mechanism of the form

Table 1. The values of the constant rates (k) and initial rate (V_0) of the reaction of the reduction of $Fe^{3+}(MGD)_2$ complexes (100 μM) with L-cysteine or glutathione and the reaction of oxidation of $Fe^{2+}(MGD)_2$ complexes (100 μM) with oxygen in intracellular medium in animal tissues.

Reductant/oxidant	Order of reaction	k	V_0 (M/s)
L-cysteine (0.1 mM)	Fours	$(4.8 \pm 0.5) \times 10^8 M^{-3}s^{-1}$	4.8×10^{-8}
Glutathione(10 mM)	Second	$(25.5 \pm 0.5)\ M^{-1}s^{-1}$	2.5×10^{-5}
Oxygen (0.03 mM)	Second	$5\times10^5\ M^{-1}s^{-1}$	1.5×10^{-3}

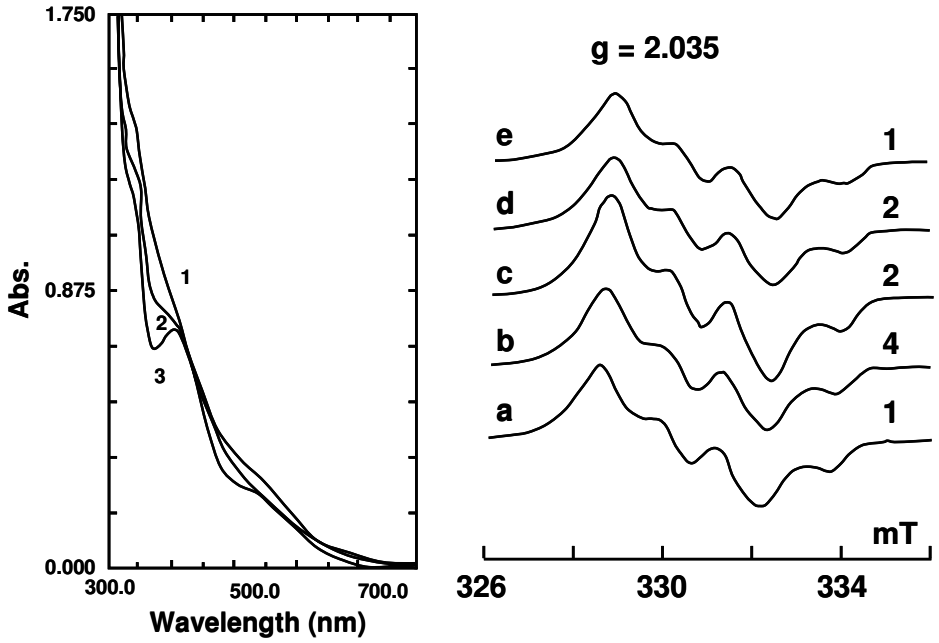

Fig.5. Optical and EPR spectra evolution of the solution of non-stable NO-$Fe^{3+}(MGD)_2$ complex in deoxygenated Hepes buffer, pH7.4. Left panel: Optical absorption spectra of the solution of 0.1 mM $Fe^{3+}(MGD)_2$ complex 1, 5 and 20 min after addition of 0.1 mM cys-NO resulting in the formation of non-stable NO- $Fe^{3+}(MGD)_2$ complex. Right panel: EPR spectra from the solution of 0.1 mM $Fe^{3+}(MGD)_2$ complex 1, 5, 10 and 20 min after addition of 0.1 mM cys-NO (spectra a-d, respectively). (e) from the solution of 0,1 mM paramagnetic NO- $Fe^{2+}(MGD)_2$ complex.. The amplifications of the EPR spectrometer in arbitrary units are shown at right side. Recordings were made at 77K.

GS-H ⟷ GS– + H+ cys– + H+

Fe3+(MGD)2 + GS– ⟶ Fe2+(MGD)2 + GS.

Scheme 3

To explain second order of the reaction in cysteine we propose that thyil radical of cysteine forms with cysteine anion very strong reductant, one-electron reduced disulfide that is capable of reducing $Fe^{3+}(MGD)_2$ complex (Scheme 2) . Thyil radical of glutathione is also combined with anion glutathione (Harman, Mottley, Houchi, Tamaka & Mason, 1984) but formed one-electron glutathione disulfide is not capable of reducing iron-MGD complex due to bulk size of the molecule.

The kinetics constants for the reduction reactions were obtained by fitting the curves of Fig.2 (see Appendix), and are presented in the Table 1. These data allowed to compare the initial rates (V_0) of the reduction of $Fe^{3+}(MGD)_2$ complexes with L-cysteine or glutathione and the reverse oxidation of $Fe^{2+}(MGD)_2$ complexes by molecular oxygen in intracellular medium in animal tissues (Table 1). Although tissue concentrations of oxygen are lower than those of thiols in intracellular medium in animal tissues (ca. 0.03 mM O_2 vs. 0.1mM of cysteine or 10 mM of glutathione; Packer & Cadenas, 1995), the two orders and more of magnitude difference in reaction rate favors the oxidation reaction by oxygen decisively. So, our data obtained demonstrate that the oxidation of $Fe^{2+}(MGD)_2$ complexes by molecular oxygen is much more efficient than the reverse reduction nitrosothiols like cysteine or glutathione in animal tissues. We conclude that the iron-carbamate complexes under physiological conditions exist in predominantly oxidized ferric state. This calls into question the conventional view on the formation of reduced nitrosyl-iron-carbamate complexes.

It is noteworthy the difference between above-described kinetics parameters and the parameters obtained for the reaction of $Fe^{2+}(MGD)_2$ reduction with cysteine or glutathione in (Tsuchiya, Yoshizumi, Houchi, Tamaka & Mason, 2002). Unfortunately, we can not discuss the difference because of absence respective experimental data in (Tsuchiya *et al*., 2002).

In addition, we considered possible reduction of complex (I) by dithionite or excess dithiols like MGD itself**.** In vessels open to ambient air, complete reduction of complex (I) in buffer was achieved within seconds by suppletion of 1 mM dithionite, whereas suppletion of an additional 2.5 mM of MGD fails to reduce the complexes noticably (data not shown).

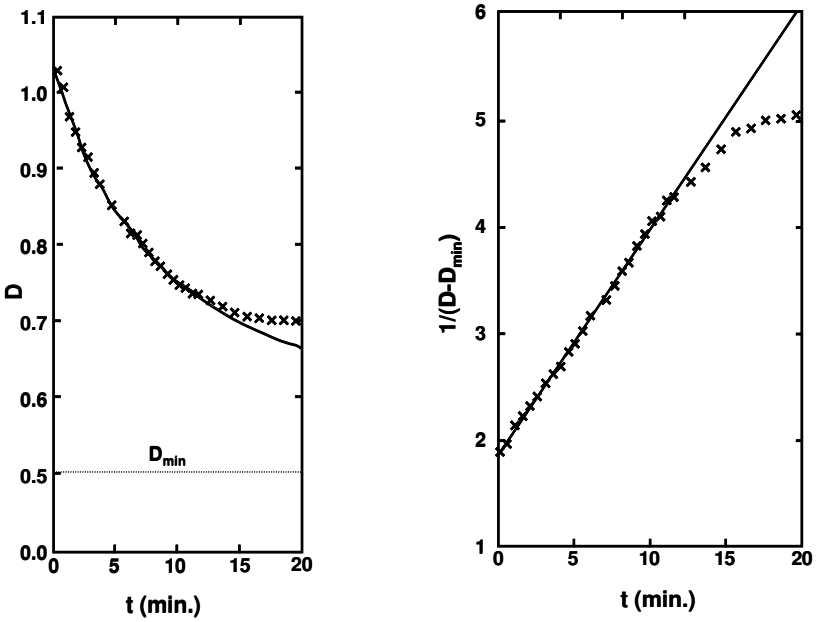

Fig.6. S-Nitrosation of MGD with cys-NO in 150 mM Hepes buffer solutions, pH 7.4. Left panel: Decrease in optical optical absorption of cys-NO (1mM) during the time. Recordings were made at every 3 min. Right panel: Stabilization of optical absorption of 1mM cys-NO solution in the presence of 1 mM MGD due to the formation of MGDS-NO. Recordings were made every 3 min.

Interaction of $Fe^{3+}(MGD)_2$ complexes with ascorbate or citrate.

Addition of ascorbate (1-10 mM) to the solutions of $Fe^{3+}(MGD)_2$ complexes (100 μM) resulted in rapid bleaching during the first few seconds that was followed by a slower process approaching a stationary level of bleaching (Fig. 3 a,c). The contribution of the rapid component is more prominent if ascorbate is increased to 10 mM, or if the MGD is decreased. However even the highest ascorbate excess concentration (10 mM) full bleaching is not achieved in anaerobic conditions. In contrast to the experiments with cysteine or glutathione, the original color of $Fe^{3+}(MGD)_2$ complexes was not recovered when the ascorbate-bleached solution was shaken in air for a few minutes (data not shown). However, full recovery was achieved when MGD concentration in the solution was increased from initial 1 mM to 5 mM (Fig. 3a). The result allows to suggest that bleaching of the solution induced by ascorbate was not due to reduction of $Fe^{3+}(MGD)_2$ complexes but probably with replacing MGD ligands by ascorbate molecules. The experiment with addition of Na-citrate (0.5 mM) to the solutions of $Fe^{3+}(MGD)_2$ complexes was in line with the proposition. Citrate also induced bleaching the solution and resulted in transformation of the absorption spectrum to that characteristic of Fe^{3+}-citrate complex (Fig.3b). The initial spectrum is restored at least partially by increasing the MGD concentration from 1 mM to 5 mM similarly to that observed in the experiments with ascorbate addition. Interestingly, when the solutions of $Fe^{3+}(MGD)_2$ complex + 1 mM MGD + 0.5 mM Na-citrate was treated with gaseous NO the spectrum characteristic of NO-$Fe^{3+}(MGD)_2$ complex (complex III) was registered (data not shown). Subsequent addition of 5 mM ascorbate led to the optical absorption characteristic of NO-$Fe^{2+}(MGD)_2$ complex (complex IY) (data not shown).

Formation and stability of NO-Fe^{3+}-MGD complexes (complexes III)

The formation of diamagnetic nitrosyl complexes (III) was observed spectroscopically when excess cys-NO was added to the solution of 0.1 mM Fe^{3+} and 1.0 mM MGD in 150 mM Hepes buffer (pH 7.4). Upon suppletion of 1.2 mM cys-NO the color changed from deep orange brown to the characteristic yellow colour of complex (III). The absorption spectrum of the complex did not change for at least 20 min (Fig. 4, Panel a). Immediately after mixing , the yellow solution gave no EPR signal at g = 2.035. Subsequently, very slow spontaneous formation of paramagnetic NO-Fe^{2+}-MGD complexes (complexes IV) was detected by drawing EPR aliquots at regular time intervals. A comparison of the EPR intensity shows that the concentra-

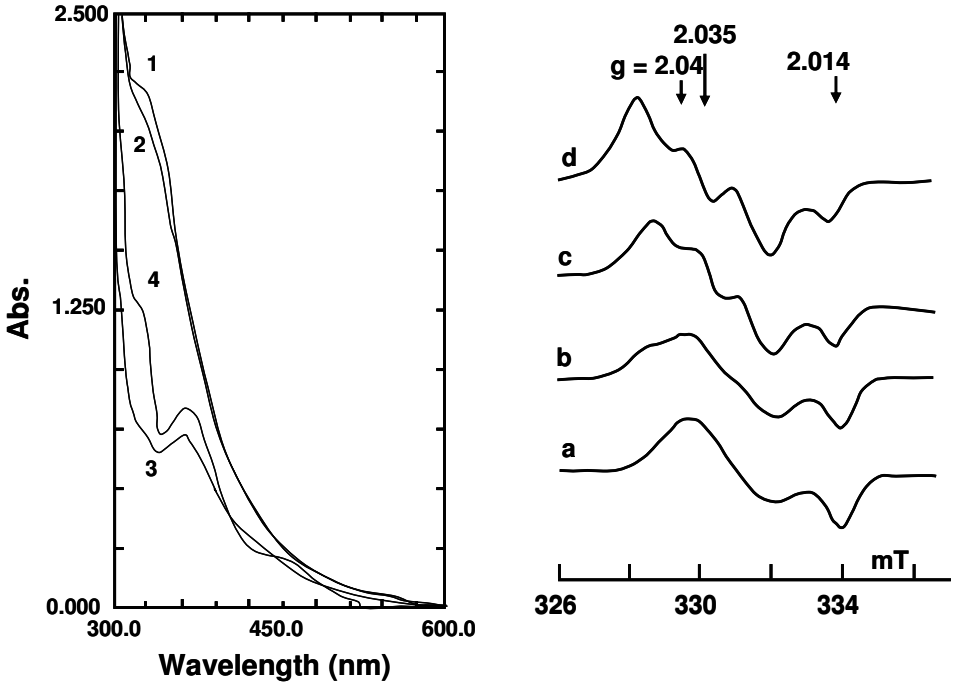

Fig.7. The kinetics curves of the reduction of stable NO- $Fe^{3+}(MGD)_2$ complex (0.1 with ascorbate (5 mM) in 150 mM Hepes buffer solution, pH 7.4. Left panel: The decrease in time in optical absorption of complex solution at 351nm after addition of ascorbate. Right panel: Linearization of the kinetics curve presented in left panel in 1/D coordinates. Crossed curves are experimental ones; solid curves are correspondent to the reaction followed with second order rate low in $Fe^{3+}(MGD)_2$ complex. The reaction proceeded at ambient temperature.

tion of complex IV reaches 1 μM after 20 min (Fig.4, panel b).

The formation of complex IV could be sharply accelerated by reinforcing the MGD content of the solution: Upon suppletion of 5 mM MGD complex IV reached to 10 μM in just 2 min (Fig.4, panel b), showing that the rate of formation was enhanced by two orders of magnitude! A comparison of the EPR intensity showed that, within experimental accuracy, all available iron (100μM) was in the form of complex IV after addition of 10 mM ascorbate (Fig.4, panel b). The color of the solution turned from yellow to deep green and the optical spectrum approached that of a solution of complex IV (Fig. 4, Panel a). It is noteworthy that these reactions proceed in fully oxygenated solutions exposed to ambient air.

Fig. 4, Panel C shows the kinetics of the nitrosylation of complex I into stable complex III under excess of cys-NO (1.2 mM). The reaction was monitored by the change of optical absorption at 514 nm. Linearization of the curve in log ($D - D_{min}$) coordinate versus time (Fig. 4, Panel D) indicates the first order of the reaction in $Fe^{3+}(MGD)_2$. D_{min} is the optical absorption of the final complex III. The reaction has several potential pathways: First, a two-step pathway where Cys-NO releases the NO radical which is subsequently trapped by complex I. This pathway I is improbable since the MGD concentration (1 mM) is sufficiently high to quench the spurious free metal ions which are needed to catalyze the release of NO. Second, a first order trans-nitrosylation reaction according to scheme 3 which leads to thiyl radicals as intermediates for disulfide bridge formation. This reaction according to Scheme 4 is compatible with our kinetic data:

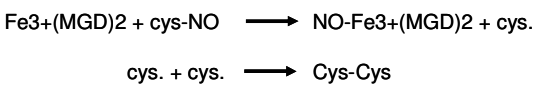

Scheme 4

By monitoring the concentration of complex (I) at 514 nm, the reaction rate constant is found to be $83 \pm 3\ M^{-1}s^{-1}$.

Alternatively, diamagnetic complexes (III) were obtained by mixing deoxygenated solutions of 0.1 mM Fe^{3+} and 1 mM MGD with NO gas in Thunberg tube followed by evacuation of NO gas from the apparatus. Exposure to gaseous NO for 1 min changed the color from deep orange brown to yellow within a few seconds. We failed to estimate

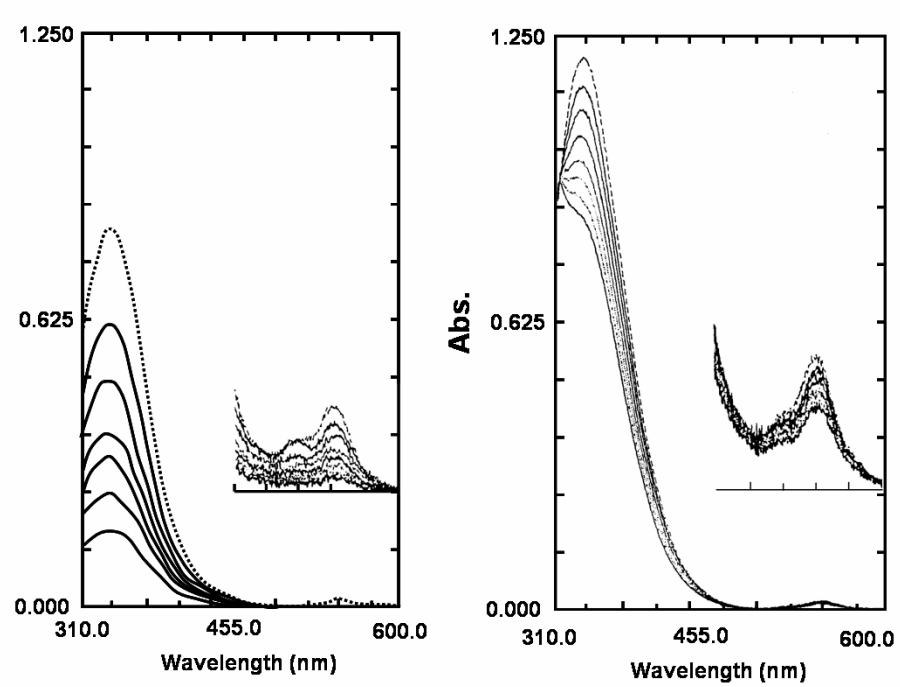

Fig.8. Optical and EPR spectra evolution from the solution of stable NO-$Fe^{3+}(MGD)_2$ complex (0.1 mM) induced with addition of 1mM cysteine in 150 mM Hepes buffer solutions, pH 7.4. Left panel: Change in optical spectra of NO-$Fe^{3+}(MGD)_2$ complex solution (curves 1,2 recorded within 10 min without cysteine addition) 1 and 20 min after cysteine addition (curves 3 and 4, respectively). Right panel: Change in EPR spectra of NO-$Fe^{3+}(MGD)_2$ complex solution 1, 10 and 20 min after cysteine addition (a-c, respectively). d) The EPR spectrum from the solution of 0,1 mM paramagnetic NO- $Fe^{2+}(MGD)_2$ complex.. The amplifications of the EPR spectrometer in arbitrary units are shown at right side. Recordings were made at 77K.

the rate constant of the process, but expect it to be close to $(4.8 \pm 0.9)\times10^8$ $M^{-1}s^{-1}$, the value quoted (Fujii, Kobayashi, Tagawa & Yoshimura, 2000) for a closely related water soluble complex with N-(dithiocarboxy)sarcosine carbamate ligands.

EPR spectroscopy on frozen aliquots (77 K) showed that 10 seconds of exposure to gaseous NO had caused the formation of a small quantity (ca 30 nM) of paramagnetic ferrous complexes (IV). However in accordance with previous data (Vanin, *et al*., 2000) prolonged exposure for 10 minutes induced a prominent color changes from yellow to green. EPR spectroscopy on frozen aliquots showed that ca. 50% of the total iron content had formed complexes IV. The remaining half was still present as complex III, because all iron was recovered as complex IV when ascorbate or dithionite were suppleted to the solution (data not shown). Interestingly, the stability of diamagnetic complex III formed in the experiments with NO treatment increased when MGD concentration in 0.1 mM Fe^{3+} solutions was diminished from 1 mM to 0.3 mM. The complex III kept stability at least 10 min after NO evacuation (data not shown).

Rapid spontaneous transformation of diamagnetic complex III to paramagnetic complex IY was also observed if cys-NO was added in much less amount (100 μM) to the solution of 100 μM Fe^{3+} and 2.5 mM MGD in 150 mM Hepes buffer (pH 7.4). The changes in optical and EPR spectra of the solutions are illustrated in Fig.5, left and right panels. The redox transformation of the complex III began immediately after mixing. After 1 min the concentration of the complex IY achived 20-25 μM and after 10 min it stabilized at the level of 50 μM. So, only half complexes III were transformed to paramagnetic state. Another part could be transformed to this state only at action of an reducing agents (Fig.5).

Interaction of stable complex III with reducing agents

The reduction experiments were performed on preparations of the stable ferric mononitrosyl complexes III in 150 mM Hepes buffer. The complexes were obtained by mixing 0.1 mM Fe^{3+} and 1mM MGD and excess 1.2 mM cys-NO. Addition of 5 mM ascorbate to the final solutions changed the

color from yellow to deep green demonstrating transformation of complexes III to complexes IV (Fig.4, Panels a and b). The left panel of Fig. 6 shows the time dependence as monitored spectrometrically at 351 nm. We find that ascorbate easily and effectively reduces the ferric mononitrosyl complex III, in stark contrast to its failure to reduce the non-nitrosylated ferric complex I. After ca. 10 minutes, the transformation of the complex III into complex IV was complete. The green solution was stable for hours under anaerobic conditions, but slowly re-oxidized to the yellow complex (III) when exposed to ambient air. The re-oxidation was accelerated by shaking the solution with air.

Linearization of kinetics curve in coordinate $1/(D - D_{min})$ versus time (Fig. 6, right panel) at least for initial 10 min of the process points to second order of the reaction in $Fe^{3+}(MGD)_2$ complex (D_{min} is the absorption characteristic of the final products of the reaction). Deviation from the second order low after 10 min could be caused by the interference from the optical absorption of an intermediate product of the reaction. Because ascorbate molecule can function as a two-electron donor it is reasonable to suggest first order of the reaction in this reductant.

The value of the initial rate of the reaction at NO-$Fe^{3+}(MGD)_2$ and ascorbate concentrations of 0.1 mM and 5 mM, respectively calculated from the kinetics curves (Fig.6) was equal to 1.8×10^{-7} M/s. As to the value of the rate constant calculated from the kinetics curves it was equal to 9×10^{6} $M^{-2}s^{-1}$.

L-cysteine as well as glutathione could also reduce complex III completely to paramagnetic complex IV. However optical and EPR data showed that the formation of complex IV by thiols proceeded via a complex mechanism, and certainly not via straightforward reductive electron transfer from thiol molecule to the iron center. The reaction with L-cysteine has been closely scrutinized: Suppletion of 1 mM L-cysteine to a buffered 0.1 mM solution of stable complex III first induced the rapid (within 30 s) formation of transient paramagnetic species which was identified as **a** dinitrosyl iron complex with cysteine (DNIC-cysteine, formula $(cys^-)_2Fe^+(NO^+)_2$) (Vanin & Kleschyov, 1998). These DNIC intermediates including practically all iron from the solution may be observed by EPR and optical spectroscopy (Fig. 7, left and right panels). Their subsequent decay on a timescale of ca. 20 min. is accompanied by the appearance of paramagnetic complex IV (Fig.8, left panel, curve 3). A slower version of this sequence was observed if glutathione was supplied instead of cysteine (data not shown). This transformation of DNIC

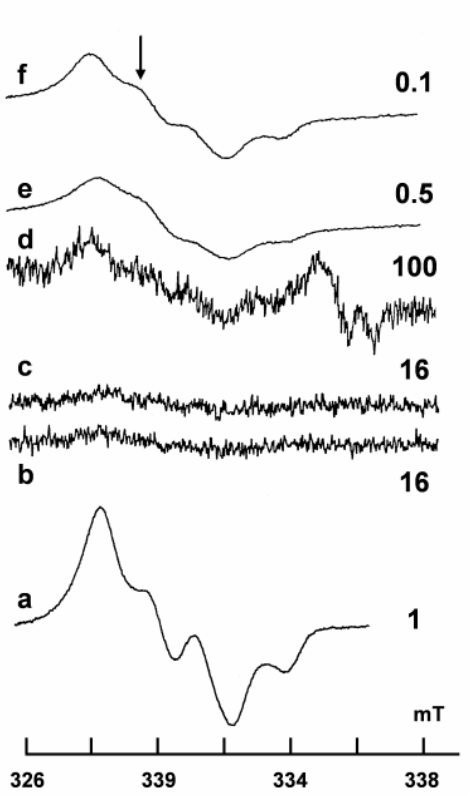

Fig.9. Nitrite as a NO donor for paramagnetic NO-$Fe^{2+}(MGD)_2$ complex formation (EPR assay). 1.5 mM $NaNO_2$ is incubated with 2.5 mM MGD + 0.5 mM Fe^{3+} for 20 min (b) in distillate water (pH 6.0) + 20 mM ascorbate; (c) in 10 mM phosphate buffer (pH 7.4) + 20 mM ascorbate; (d) in 150 mM Hepes buffer (pH 7.4) + 10 mM dithionite; (e) in 10 mM phosphate buffer (pH 7.4) + 10 mM dithionite; (f) in distillate water + 10 mM dithionite. (a) The EPR spectrum from the solution of 0,1 mM paramagnetic NO- $Fe^{2+}(MGD)_2$ complex. The amplifications of the EPR spectrometer in arbitrary units are shown at right side. Recordings were made at 77K.

intermediates proceeded in deoxygenated as well in oxygenated solutions**.** In accordance with data, described in Vanin, Liu, Samouilov, Stukan & Zweier, 2000 long term exposure to ambient air or shaking in air (within 1-2 hrs) led to decrease the amount of complex IY that was accompanied the appearance of complex I. As to complex III it rapidly (for a few minutes) transformed into complex I in air (data not shown).

Trans-nitrosation reaction between cys-NO and MGD

As above demonstrated cys-NO is capable of nitrosating $Fe^{3+}(MGD)_2$ complexes by donating NO molecule that results in complex III formation (Scheme 4). It is reasonable to suggest that the process is accompanied with S-nitrosation of free MGD molecules with cys-NO. Earlier such type of

the reaction was observed for diethyldithiocarbamate (Arnell, Day & Stamler, 1997). The experiment supported the idea. The S-nitrosation of MGD molecules was studied spectrophotometrically. Solutions of 1mM cys-NO in 150 mM Hepes buffer, pH 7.4 showed a characteristic absorption bands at 340 and 540 nm (Fig. 8, left panel) as described elsewhere (Williams. 1985). Decrease in intensity of the bands during the time demonstrated low stability of cys-NO in the solution. The compound degraded completely for half hour. The addition of 1 mM MGD attenuated the process (Fig. 8, right panel). Moreover the stabilization of the intensities of both absorption bands was observed at the level of 0.6 mM RS-NO. Small shift of the band at 340 nm to lower wave length and transformation of the shape of the absorption band at 540 nm allow suggesting that the effect was due to the formation of stable S-nitroso-MGD (MGD-SNO) compound.

Nitrite does not induce formation of complex IV in 150 mM Hepes buffer solutions

Reduction of nitrite to nitric oxide is a well known reaction pathway under acidic conditions. We investigated the possibility of such artificial NO release by using EPR to detect the formation of paramagnetic complexes (IV) in various aqueous solutions containing 1.5 mM $NaNO_2$, [MGD]=2.5 mM and [Fe^{3+}]= 0.5 mM. During 20 minutes of incubation, 20 mM of ascorbate generated less than 30 nM of complex (IV) in distillate water (pH = 6.0), 10 mM PBS (pH 7.4) or 150 mM HEPES buffer (pH 7.4 (Fig. 9). In contrast, far higher levels of complex (IV) were produced by 10 mM dithionite in unbuffered or weakly buffered solutions. After five minutes, the yields were 200 μM in distillate water and 40 μM in the mildly buffered 10 mM PBS (pH 7.4) (Fig.9). The yield was proportional to the initial nitrite concentration and reflects the NO release due to the reduction of nitrite under acidic conditions. We verified that the suppletion of 10 mM dithionite induced acidification of the weak PBS buffer. In contrast, NO release remains negligible when the reduction is carried out in a strong buffer: No complex IV was detected when 10 mM dithionite was added to solutions in a strong 150 mM HEPES buffer, pH 7.4 (Fig. 9) . The yield increased to 80 nM when massive 100 mM dithionite was added.

Endogenous nitrite levels in biological systems are estimated to be in the range of 1-20 μM (Rodriguez, Maloney, Rassaf, Bryan & Feelish, 2003), ca. three orders of magnitude below the mM nitrite concentration used here. Our data show that ascorbate and dithionite can be safely used for the reduction of complex (III) to (IV) if the buffering is adequate to prevent acidification. In particular, the reduction does not significantly distort the adduct yield by the artificial release of NO from nitrite. This conclusion is highly relevant for NO detection by iron-dithiocarbamate methods as described in the following paragraph.

Effect of dithionite e treatment on the yields of complex IV in mice tissues

The effect of reduction on yields of paramagnetic complex IY was investigated in mice pretreated with LPS as a model for acute infection. Fig 10 gives representative EPR spectra from frozen liver and kidney samples before and after suppletion of dithionite. Unreduced EPR spectra appear as the superposition of complex IV (g = 2.035) and several undesirable background signals from other paramagnetic species. The most prominent contamination is the Cu^{2+}-DETC (S=1/2) complex often observed in animal tissues. Its spectrum is characterized with 4 components a, b, c and d from the hyperfine interaction with the Cu^{2+} (I=3/2) nucleus. Other contaminants are a wide anisotropic EPR line attributed to Hb-NO (g = 2.07, 1.98), a free radical signal at g = 2.0 and the EPR signal of reduced iron-sulfur proteins (g = 1.94).

Table 2 shows that the yields of complex IV in

Table 2. Influence of dithionite treatment on the yields of paramagnetic complex IV in tissue preparations from mice pre-treated with LPS for 4 hr.s, Incubation with Fe-DETC traps was 10 or 30 min. Reduction of tissue samples was by incubation with 10 mM dithionite for 30 minutes. Fe+DETC were added to animals for 10 min. for 30 min. The amount of paramagnetic MNIC-DETC (μM/kg).

Tissue preparation	-dithionite	+dithionite	-dithionite	+dithionite
liver	2±1	12±3	12±4	33±9
kidney	0.5±0.2	3±1	3±1	7±3
heart	0.3±0.1	2±1	0.8±0.3	2±1
spleen	0.4±0.2	1.0±0.5	1.0±0.5	2±1
lung	0.4±0.2	1.0±0.5	2±1	4±2

various organs of mice are sharply increased by dithionite treatment (Table 2). The increase in the yields can be seen both at short incubation of 10 min and longer incubation of 30 min. At short incubations of just 10 minutes, the reductive enhancement is particularly prominent in liver, kidney and heart tissues. Overall yields can still be enhanced considerably by extending the incubation time to 30 min.

Incubation with 10 mM dithionite for 30 minutes resulted in the disappearance of Cu^{2+}-DETC signal and increasing Hb-NO signal in some preparations (heart, spleen, lung) (data not shown). The reduction of the unwanted Cu^{2+}-DETC contaminations greatly facilitated the quantification of the tissue yields of complex IV.

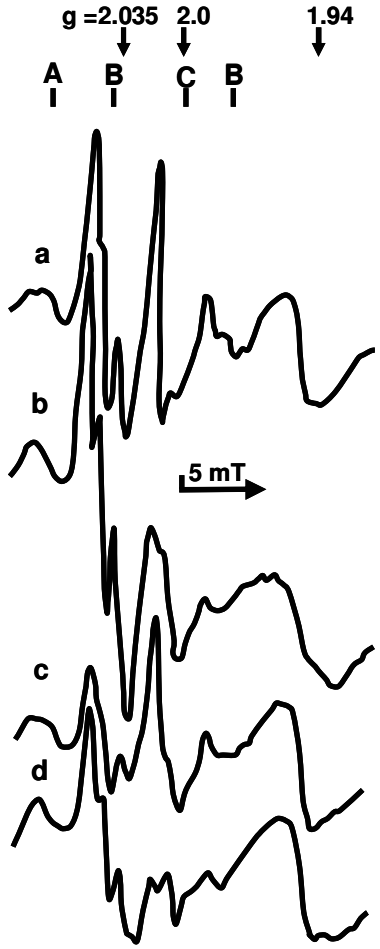

Fig.10. NO trapping in liver or kidney of mice, treated with LPS (4 hrs) followed with injection of Fe-DETC to mice for 30 min. EPR assay.liver; (b) preparation (a) + 10 mM dithionite in 150 mM Yepes buffer, pH7.4; kidney; (d) preparation (c) + 10 mM dithionite in 150 mM Hepes buffer, pH 7.4. Recordings were made at 77K at identical amplifications of radiospectrometer.

DISCUSSION

The main results of the present investigation can be summarized as follows:

1. Endogenous biological reductants like (in anionic state) have very modest reaction rates for the reduction of complex I to ferrous complex (II). The reaction proceeds by one-electron transfer. The reaction rates are at least two orders of magnitude slower than the reverse oxidation by molecular oxygen in intracellular medium in animal tissues (Table 1).
2. In solution, exposure to freely diffusing NO efficiently nitrosylates Fe^{3+}-MGD (complex I) to diamagnetic complex III . Transnitrosylation of Fe^{3+}-dithiocarbamates by cys-NO is an alternative and efficient pathway for the formation of the diamagnetic nitrosyl complex (III). It should be noted that the nitrosyl group is transferred as NO, and not in the form of NO^+ similarly to that for Fe^{2+}-MGD (Butler, Elkins-Daukes, Parkin & Williams, 2001; Vanin, Papina, Serezhenkov & Koppenol, 2004).
3. The nitrosylated complex (III) is far easier to reduce than its non-nitrosyl counterpart (I). For example, the nitrosylated complex III is efficiently reduced by ascorbate, whereas complex (I) is not**.** In principle, biological thiols like cysteine or glutathione are also capable of reducing complex III, but the process can proceeds via a complex mechanism involving paramagnetic dinitrosyl-iron complexes as intermediates. The ensuing nitrosylated adduct (IV) is far more stable against oxidation by oxygen than its non-nitrosyl counterpart (II).
4. The diamagnetic complex III can be maintained in stable state when synthesized from complex I in presence of excess cys-NO. When synthesized at low amount of cys-NO the complex III spontaneously transforms to complex IY evidently through the mechanism of reductive nitrosylation that is accompanied with the accumulation of S-nitrosylated dithiocarbamate molecules. Upon suppletion of iron-carbamate traps to living systems, trapping of endogenous NO leads to the formation of mononitrosyl-iron complexes. These complexes are a mixture of ferric and ferrous charge state. In all bio-

logical systems scrutinized here, the redox equilibrium is firmly on the diamagnetic ferric side. The yield of the paramagnetic ferrous complex IY in animal tissues may be enhanced considerably by reduction with dithionite.

The first result shows that the dominant endogenous reducing agents cysteine or glutathione have only modest capacity to reduce ferric dithiocarbamate complexes. The data presented in Table 1 demonstrate that the rates of this reaction at least two orders of magnitude less than the reaction rate for oxidation of $Fe^{2+}(MGD)_2$ with oxygen in intracellular medium in animal tissues. As to hydrophobic iron-DETC complexes localized in membrane cell compartments the hydrophylic features of cysteine or glutathione make difficult the reduction of these complexes. In contrast, oxygen molecules are capable of membrane penetrating thereby ensuring the oxidation of Fe-DETC complexes. That allows to argue that the overwhelming majority if not all of NO traps remain in oxidized state under physiological conditions. Clearly, the conventional counterclockwise pathway in the Scheme 1 is not feasible. Phrased otherwise, the actual trapping of NO is achieved by the ferric complex (I) and the formation of paramagnetic adducts proceeds via the nitrosylated intermediate complex (III). The data demonstrating similarity between the values of the rate constants of the nitrosylation reaction of Fe^{2+} or Fe^{3+}-dithiocarbamate complexes (Fujii *et al*., 2000) are in line with the proposition. In terms of diagram 1, our data show that the formation of paramagnetic adducts is dominated by the clockwise pathway. We note that our mechanism is at odds with the conventional viewpoint. It is noteworthy here that conventional using Fe^{2+} salts for preparing iron stock solution is well founded due to better water solubility of these salts as compared with that of ferri salts. Nevertheless, when Fe^{2+} ions combine with dithiocarbamate ligands their complexes are easily oxidized by oxygen in biosystems.

Results 2 and 3 are in lines with previous data (Vanin *et al*., 2000) that $Fe^{3+}(MGD)_2$ may bind NO even when in oxidized state. The NO may come from freely diffusing NO radicals in solution as well as abstracted from low molecular weight S-nitrosothiols like cys-NO or GS-NO. Free NO has high mobility and is trapped with rates orders of magnitude faster than the transnitrosylation reaction with Cys-NO. A similar situation applies to the trapping of NO by ferrous $Fe^{2+}(MGD)_2$ complexes (Butler, Elkins-Daukes, Parkin &Williams, 2001; Vanin, Papina, Serezhenkov & Koppenol, 2004)

The analysis of Result 4 points to important role of the process of reductive nitrosylation of the complex III for its stability. Dithiocarbamate molecules can initiate the process as followed from Scheme 5 demonstrating the proposal mechanism of the formation of final complex IY from complex III at the participation of S-nitrosothiols (RS-NO), cys-NO or GS-NO as a NO donors. RS-NO molecules are added in the amount equal to that of $(MGD)_2Fe^{3+}$complexes.

$$MGD_2Fe^{3+} + RS\text{-}NO \rightarrow MGD_2Fe^{3+}\text{-}NO + RS\cdot$$

$$MGD_2Fe^{3+}\text{-}NO \leftrightarrow MGD_2Fe^{2+}\text{-}NO^{+}$$

$$MGD\text{-}S^{-} + MGD_2Fe^{2+}\text{-}NO^{+} \rightarrow MGD_2Fe^{2+} - SNO$$

$$MGD_2Fe^{2+} + MGD_2Fe^{3+}\text{-}NO \rightarrow MGD_2Fe^{2+}\text{-}NO + MGD_2Fe^{3+}$$

Scheme 5

According with the Scheme 5, the $(MGD)_2Fe^{2+}$-NO^+ complex donates NO^+ ion to MGD molecule resulting the appearance of $(MGD)_2Fe^{2+}$ complex. The latter accepts consequently NO molecule from $(MGD)_2Fe^{3+}$-NO complex forming more stable $(MGD)_2Fe^{2+}$-NO complex (complex IY). As a result NO molecules from cys-NO are equally distributed between complex IY and MGD-SNO.

Similar mechanism can operate for complex IY formation at participation of NO instead of RS-NO. The mechanism reminds that of reductive nitrosylation of nitroso ferriheme complexes (Hoshino, Maeda, Konishi, Seki & Ford, 1995). Higher affinity of thiol-containing compounds to nitrosonium ions (NO^+) (Wink, Nims, Darbyshire, Christodolou, Handbauer, Cox, Laval, Laval, Coon, Krishna, deGraat & Mitchel, 1994) than that of hydroxyl anions allows to consider MGD molecules as a main acceptor of NO^+ ions in the system. This is the main distinction of proposed mechanism of reductive nitrosylation from that characteristic of nitrosyl heme-iron complexes (Hoshino, Maeda, Konishi et al, 1995).

The data presented in Fig.5 are consistent with Scheme 5. When cys-NO or NO molecules were added to the solutions of $Fe^{3+}(MGD)_2$ complexes in the amount equal to that of the complexes only 50% of iron was found in paramagnetic complex IY). The fact allows to suggest that distinctly from cys-NO or GS-NO S-nitrosylated MGD molecules accumulated in accordance with Scheme 5 are not capable of nitrosylation of iron-MGD complexes. That correlates with high stability of MGD-SNO molecules (Fig.6). Addition of ascorbate or dithionite leads to N**O** release from the molecules that results to all iron including into the complex IY.

In the presence of excess of cys-NO MGD molecules could be S-nitrosylated through the reaction of S-transnitrosylation. The process was demon-

strated directly spectrophotometrically (Fig.8). S-nitrosylation of MGD molecules could make the deficiency of free thiol-containing MGD molecules initiating the process of reductive nitrosylation of complex III thereby ensuring the stability of the complex. Similarly the stable complex III could be synthesized by gaseous NO treatment of the solution of complex I at low ratio of iron and MGD. Subsequently the process could be induced by addition of MGD molecules (Fig. 4).

Thus, the reaction of NO molecules, cys-NO or GS-NO as a NO donors with complex I can produce the populations of compounds: diamagnetic complex III, paramagnetic complex IY and MGD-SNO molecules. What the situation can be characteristic of these populations in animal or plant cells and tissues? Evidently endogenous reductants like ascorbate can sharply diminish the level of complex III and MGD-SNO resulting in the accumulation of complex IY. The presence of these endogenous reductants is a plausible explanation of the success of in vivo trapping of NO with iron-dithiocarbamate complexes. However, the experiments with treatment of isolated animal tissues with dithionite show that the effect of endogenous reductants not so efficient. The main part of the compounds from above-mentioned populations remains in EPR-silent state in the tissues. It means that complexes III and S-nitrosylated dithiocarbamate molecules are in majority. Our data do not allow to estimate the contribution of these compounds in "EPR-silent" population. The problem remains obscure and needs in further investigation. In particularly, the effect of superoxide ions and peroxynitrite transforming paramagnetic complex IY into EPR-silent state (Vanin, Huisman, Stroes, de Ruijter-Heijstek, Rabelink & van Faassen, 2001) should be also studied. We can only guarantee that endogenous nitrite as a possible NO donor did not make any notable contribution to the process. As shown above using strong buffer solutions at pH 7.4 in the experiments prevented the contribution. Thus the experiments demonstrate that the treatment of animal cells or tissues with endogenous reductants can significantly increase the efficiency of the iron-dithiocarbamate method of NO detection in biosystems.

It is noteworthy here that the beneficial effect of dithionite on adduct yield has observed before (Mulsh, Vanin, Mordvintcev, Haushildt & Busse, 1992; Tsuchiya, Tagasugi, Minakuchi & Fukuzawa, 1996) in tissue preparations of test animals. However, these early observations can be wholly or partially attributed to the artifact of reduction of nitrite. Our results demonstrate that artifacts from nitrite may be avoided by preventing acidification, for example by reducing the tissue preparations in presence of strong buffers.

The formation pathway of complex (IV) with N-(dithiocarboxy) sarcosine (DTCS) ligands has been investigated previously by Yoshimura and co-workers (Fujii, Kobayashi, Tagawa & Yoshimura, 2000). The authors propose a clockwise two-step mechanism. The first is straightforward NO trapping by complex (I), followed by a new mechanism to reduce complex III reduction by disulfide formation. In this mechanism, the DTCS ligands are presumed to have reductive capacity, the net reaction being

$$2Fe^{3+}(DTCS)_3 + NO \rightarrow NO\text{-}Fe^{2+}(DTCS)_2 + Fe^{3+}(DTCS)_3 + \tfrac{1}{2}\,\text{DTCS disulfide}$$

Scheme 6

The process was observed at low amount of NO and high excess of $Fe^{3+}(DTCS)_3$. These conditions do not apply to our experiments when the quantities of cys-NO exceed those of Fe^{3+}-MGD, nor to situations encountered in animal tissues during trapping experiments. Therefore, we feel that reactions like scheme 6 do not significantly contribute to the formation of paramagnetic adducts in actual trapping experiments.

The nitroxyl ion NO^- has been proposed (Xia, Cardounel, Vanin & Zweier, 2000) as an alternative potential source of paramagnetic adducts by reacting directly with the ferric Fe^{3+}-MGD(DETC) complex. However, this proposal would be compatible with our observation that the mononitrosyl complexes in biological materials are a mixture of ferric and ferrous forms as well as S-nitrosylated dithiocarbamate molecules. In contrast, nitrosylation of Fe^{3+}-MGD(DETC) complex by nitroxyl ions as dominant pathway could result only the formation of paramagnetic complex IY. In generally, this idea is at odds with a myriad of observations on MNIC formation by NO in unambiguous neutral radical state (e.g. when supplied by true NO donors, gaseous NO, or identified with NO electrodes).

In conclusion, we have considered the pathway of complex IY formation through the reaction between $Fe^{3+}(MGD)_2$ complex and NO (RS-NO) followed with reduction of forming complex III to complex IY. However this process can proceed without strong iron ligands like citrate anion. According to afore described data he latter can accept iron from iron-MGD complexes. In a result addition of NO (RS-NO) molecules to the system can lead to the formation of nitrosyl iron complex with citrate ligand followed with replacing citrate

ligands in the complex with MGD molecules. That results in the formation of more stable MNIC-MGD complex. This proposal mechanism is under study now in our Laboratory.

Acknowledgements

A.F.V. would like to thank the Debye Institute of Utrecht University for the hospitality during the summer of 2003 and spring of 2004. He gratefully acknowledges financial support from the Dutch Foundation for Scientific Research NWO (grant NB 90-187) and from the Russian Foundation for Basic Research (Grant 02-04-48456). We are grateful to Timmo van der Beek for the synthesis of MGD and Dr. Albert Huisman (Utrecht Medical Center) for his assistance with experiments.

REFERENCES

Arnell D.R., Day B.J. & Stamler J.S. (1997). Diethyl dithiocarbamate-induced decomposition of S-nitrosothiols, *Nitric Oxide:Biol&Chem*. **1**, 56-64.

Butler A.R., Elkins-Daukes S., Parkin D. & Williams D.L. (2001). Direct NO group transfer from S-nitrosothiols to iron centres, *Chem Commun (Camb)*. 18, 1732- 1733.

Fujii S. Kobayashi K., Tagawa S. & Yoshimura T, (2000). Reaction of nitric oxide with iron(III) complex of N-(dthiocarboxy)sarcosine: a new type of reductive nitrosylation involving iron(IY) as an intermediate. *J.Chem Soc., Dalton Trans*., 3310-3315.

Halliwell B. & Gutteridge J.M.C. (1999). [chapter title] [In:] Halliwell B. & Gutteridge J.M.C. (Eds.) *Free radicals in biology and medicine* (pp. 202-204). Oxford: Univ. Press.

Harman L.S., Mottley C. & Mason R.P. (1984). Free radical metabolites of L-cysteine oxidation. *J.Biol. Chem.*, **259**, 5606-5611.

Hoshino M., Maeda M., Konishi M., Seki H. & Ford P.C. (1995). Studies on the reactionmechanism for reductive nitrosylation of ferrihemoproteins in buffer solutions. *J. Am. Chem Soc*., **118**, 5702-5707.

Lai C.-S. & Komarov A.M. (1994). Spin trapping of nitric oxide production in vivo in septic- shock mice. *FEBS Lett*., **345**, 120-124.

Mikoyan V.D, Kubrina L.N., Serezhenkov V.A, Stukan R.A. & Vanin A.F. (1997). Complexes of Fe^{2+} with diethyldithiocarbamate or N-methyl-D-glucamine dithiocarbamate as traps of nitric oxide in animal tissues: comparative investigations. *Biochim. Biophys. Acta*, **1336**, 225-234.

Mulsch A., Vanin A., Mordvintcev P., Hauschildt S., Busse R., (1992) NO accounts completely for the oxygenated nitrogen species generated by enzymatic L-arginine oxygenation, *Biochem. J.* 288, 597-603.

Packer L. & Cadenas E. (Eds.) (1995). *Biothiols in health and disease*. N-Y/Basel/Hong Kong: Marcel Dekker.

Rodriguez J., Maloney R.E., Rassaf T., Bryan N.S. & Feelisch M. (2003) Chemical nature of nitric oxide storage forms in rat vascular tissue, *Proc. Natl. Acad. Sci. USA* 100, 336-341.

Shinobu L.A., Jones S.G. & Jones M.M., (1984) Sodium N-methyl-D-glucamine dithiocarbamate and cadmium intoxication. *Acta Pharmacol. Toxicol*. 54, 189-194.

Tsuchiya K., Takasugi M., Minakuchi K. & Fukuzawa K, (1996) Sensitive quantitation of nitric oxide by EPR spectroscopy, *Free Rad.Biol.Med*. 21, 733-737.

Tsuchiya K., Jiang J.J., Yoshizumi M., Tamaki T., Houchi H., Minakuchi K., Fukuzawa K. & Mason R.P (1999) Nitric oxide-forming reactions of the water soluble nitric oxide spin-trapping agent, MGD, *Free Rad.Biol.Med.* 27, 347-355.

Tsuchiya K., Yoshzumi M., Houchi H., Tamaka T. & Mason R.P. (2002) The role of thiol and nitrosothiol compounds in the nitric oxide-forming reaction of the iron-N-methyl-D-glucamine dityhiocarbamate complex, *Biochem. J*. 367, 771-779.

Vanin A.F., Mordvintcev P.I. & Kleschyov A.L. (1984). Appearance of nitric oxide in animal tissues, *Studia biofizika* 102, 135-143.

Vanin A.F. & Kleschyov A.L. (1998). EPR studies and biological implications of nitrosyl nonheme iron complexes, In: S. Lukiewicz, J.L. Zweier, eds. *Nitric oxide in transplant rejection and anti-tumor defense*. Kluwer Acad. Publishers 50-55

Vanin A.F., (1999) Iron diethyldithiocarbamate as a spin trap for nitric oxide detection, *Methods in Enzymol*. 301, 269-279.

Vanin A.F., Liu X, Samouilov A., Stukan R.A. & Zweier J.L. (2000). Redox properties of iron-dithiocarbamate and their nitrosyl derivatives: implications for their use as of nitric oxide in biological systems, *Biochim. Biophys. Acta* 1474, 365-377.

Vanin A.F., Huisman A., Stroes E.S.G., de Ruijter-Heijstek F.C., Rabelink T.J. & van Faassen E.E. (2001). Antioxidant capacity of mononitrosyl-iron-dithiocarbamate complexes: implications for NO traping, *Free Rad. Biol Med.* 30, 813-824

Vanin A.F., Huisman A. & van Faassen E.E. (2002) Iron dithiocarbamate as spin trap for nitric oxide detection: pitfalls and successes, *Methods in Enzymol*.359, 27-42.

Vanin A.F., Muller B.,. Alencar J.L,. Lobysheva I.I, Nepveu F.& Stoclet J.-C. (2002). Evidence that intrinsic iron but not intrinsic cooper determines S-nitrosothiol decomposition in buffer solution, *Nitric Oxide:Biol.&Chem.* 7, 194-209

Vanin A.F., Svistunenko D.A., Mikoyan V.D., Serezhenkov V.A., Fryer M.J., Baker N.R. & Cooper C.E., (2004). Endogenous superoxide production and the nitrite/nitrate ratio control the concentration of bioavailable free nitric oxide in leaves, *J. Biol. Chem* 279, 24100-24107.

Vanin A.F., Papina A.A., Serezhenkov V.A. & Koppenol W.H. (2004) The mechanism of S-nitrosothiol decomposition catalyzed by iron, *Nitric Oxide:Biol&Chem*.10, 60-73.

Williams D.L.H. (1985) S-nitrosation and the reactions of S-nitrosocompounds, *Chem Soc. Rev.*14, 171-196.

Wink, D.A., Nims R.M., Darbyshire J.F., Christodoulou D., Handbauer I., Cox G.Q., Laval F., Laval J., Coon J.A., Krishna M.C., deGraat W.G &, Mitchel J.B. (1994) Reaction kinetics for nitrosation of cisteine and glutathione in aerobic nitric oxide solutions at neutral pH. Insights into the fate and physiological effects in intermediates generated in the NO/O_2 reaction, *Chem Res. Toxicol.* 7, 5129-5125.

Xia Y. Cardounel A.J., Vanin A.F. & Zweier J.L. (2000) Electron paramagnetic resonance spectroscopy with N-methyl-D-glucamine dithiocarbamate iron complexes distinguishes nitric oxide and nitroxyl anion in a redox-dependent manner: applications in identifying nitrogen monoxide products from nitric oxide synthase, *Free Rad. Biol. Med.* 29, 793-797.

APPENDIX

The analysis of equilibrial characteristics of Fe^{3+} - MGD complex

The formation of Fe^{3+} - MGD complex above studied can be described as two-step process: The first step is Fe^{2+}binding with MGD followed with subsequent oxidation of formed $Fe^{2+}(MGD)_2$ complex with oxygen (second step):

$$Fe^{2+} + 2MGD \xleftrightarrow{K_1} Fe^{2+}(MGD)_2 \quad (1)$$

$$Fe^{2+}(MGD)_2 + O_2 + H_2O + (n-1)MGD \rightarrow Fe^{3+}(MGD)_n + H_2O_2 + OH^- \quad (2)$$

$$Fe^{3+}(MGD)_n \xleftrightarrow{K_1} Fe^{3+} n MGD \quad (3)$$

Equilibrial amount of $Fe^{3+}(MGD)_n$ complexes derived from equation 3 is described as

$$[Fe^{3+}(MGD)_n] = [Fe^{2+}]_0 / (1 + 1/K_2[MGD]^2) \quad (4)$$

or for optical absorption of $Fe^{3+}(MGD)_n$ complex at 385 nm the equation is described as

$$D_{385} = \varepsilon_{385}[Fe^{2+}]_0 / (1 + 1/K_2[MGD]^n) \quad (5)$$

where K_1 and K_2 are an equilibrium constants; n is the number of MGD ligands in the ferric complex; $[Fe^{2+}]_0$ is the initial amount of ferro ions and ε_{385} is the extinction coefficient of $Fe^{3+}(MGD)_n$ complex at 385 nm. Linearization of the equation 5 in coordinates $1/[Fe^{3+}(MGD)_n]$ and $1/[MGD]^n$ for the experimental dependence $[Fe^{3+}(MGD)_n]$ from $[MGD]^n$ (Fig. 1a, inset) was arrived at $n = 2$ (data not shown). It means that only two MGD ligands include into ferric-MGD complexes. The analysis of the curve presented in Fig.1a, inset with less squares method in accordance with equation 5 gives the value of K_2 or ε_{385} equal to 1.6×10^7 or 9335 1/M, respectively.

2. Estimation of the values of rate constants for the reactions of reduction of $Fe^{3+}(MGD)_2$ complex with glutathione (Glu) or L-cysteine (Cys).

In accordance with data obtained the reactions of $Fe^{3+}(MGD)_2$ complex reduction with glutathione (Glu) or L-cysteine (Cys) are described as k_{red}

$$Fe^{3+}(MGD)_2 + Glu - S^- \xleftrightarrow{K_a} Fe^{2+}(MGD)_2 + Glu - S \quad (6a)$$

$$Glu - SH \longleftrightarrow Glu\text{-}S^- + H^+ \quad (6b)$$

or k_{red}

$$2Fe^{3+}(MGD)_2 + 2Cys\text{-}S^- \xleftrightarrow{k_{red}} 2Fe^{2+}(MGD)_2 + Cys\text{-}Cys \quad (7a)$$

$$Cys\text{-}SH \xleftrightarrow{K_a} Cys\text{-}S^- + H^+ \quad (7b)$$

where k_{red} or K_a are the rate constants or the equilibrium constants for the process of protonization(deprotonization) of thiol group of glutathione or L-cysteine.

Having in mind first order in $Fe^{3+}(MGD)_2$ for the reaction 6a the change in complex amount in time can be described as

$$[Fe^{3+}(MGD)_2] = [Fe^{3+}(MGD)_2]_0 \exp\left\{\frac{-k_{red}[Glu\text{-}SH]_0 t)}{1 + [H^+]/K_a}\right\} \quad (8)$$

where $[Fe^{3+}(MGD)_2]_0$ or $[Glu\text{-}SH]_0$ are initial concentrations of the complex or Glu-SH, respectively. The latter was much more than that of the complex in the experiments. Linearization of the dependence 8 in ln $[Fe^{3+}(MGD)_2]$ coordinate versus time (t) characteristic also for the experimental dependence expressed in optical absorption of the complex (Fig. 2 b,e) allows to estimate the value of k_{red} from the equation:

$$k_{red} = tg\alpha \cdot (1 + [H^+]/K_a)/[Glu\text{-}SH]_0 \quad (9)$$

where α is a angle characteristic of the dependence of ln $[Fe^{3+}(MGD)_2]$ versus time.

Initial rate of the reduction of the complex was estimated as

$$V_0 = tg\alpha \cdot [Fe^{3+}(MGD)_2]_0 \quad (10)$$

Keeping in mind second order in $Fe^{3+}(MGD)_2$ for the reaction 7a the change in complex amount in time can be described as

$$[Fe^{3+}(MGD)_2] = \left\{ \frac{1}{[Fe^{3+}(MGD)_2]_0} + \frac{-k_{red}[Cys\text{-}SH]^2 t)}{1+[H^+]/K_a} \right\}^{-1} \quad (11)$$

Linearization of the dependence 11 in 1/ $[Fe^{3+}(MGD)_2]$ coordinate versus time (t) characteristic also for experimental dependence expressed in optical absorption of the complex (Fig.2a,d) allows to estimate the value of k_{red} from the equation

$$k_{red} = tg\alpha \cdot (1+[H^+]/K_a)/[Cys\text{-}SH]^2 \quad (12)$$

where α is a angle characteristic of the dependence of $1/[Fe^{3+}(MGD)_2]$ versus time.

Initial rate of the reduction of the complex was estimated as

$$V_0 = tg\alpha \cdot [Fe^{3+}(MGD)_2]_0^2 \quad (13)$$

3. Estimation of rate constant for the reaction between $Fe^{3+}(MGD)_2$ and Cys-NO leading to the formation of stable NO-$Fe^{3+}(MGD)_2$ complex ([cys-NO]>> [$Fe^{3+}(MGD)_2$])

$$Fe^{3+}(MGD)_2 + cys\text{-}NO \xrightarrow{k} NO\text{-}Fe^{3+}(MGD)_2 + cys \quad (14)$$

Both ferri complex and its nitrosylated adduct are characterized with intensive optical absorption at the diapason of 300-500 nm in the solution (Fig.1).What is why proceeding from the first order of the rate constant in $Fe^{3+}(MGD)_2$ complex for the reaction the time change in optical absorption of the solution monitored at 514 nm can be described as

$$D_t = D_{min} \cdot (D_0 - D_{min}) \exp\{-k[cys\text{-}NO]t\} \quad (15)$$

where D_t, D_{min} or D_0 are total optical absoption of the solution in time $\{\varepsilon_1[Fe^{3+}(MGD)_2] + \varepsilon_2[NO\text{-}Fe^{3+}(MGD)_2]\}$, final optical absorption of the solution determined only with $NO\text{-}Fe^{3+}(MGD)_2$ complex or initial optical absorption of the solution determined only with $Fe^{3+}(MGD)_2$ complex, respectively. ε_1 or ε_2 are extinction coefficients of the optical absorption at 351 nm of the $Fe^{3+}(MGD)_2$, $NO\text{-}Fe^{3+}(MGD)_2$ complexes, respectively. Linearization of the dependence 15 in ln ($D_t - D_{min}$) versus time characteristic also for the experimental dependence expressed in optical absorption of the solution (Fig. 3 c,d) allows to estimate the k value from the equation

$$k = tg\alpha / [cys\text{-}NO]_0 \quad (16)$$

where $[cys\text{-}NO]_0$ is the initial cys-NO concentration and α is an angle characteristic of the dependence of ln ($D_t - D_{min}$) versus time.

4. NO-$Fe^{3+}(MGD)_2$ complex reduction with ascorbat

The process is described as

$$2NO\text{-}Fe^{3+}(MGD)_2 + Asc\text{-}H \xrightarrow{k_{red}} 2NO\text{-}Fe^{2+}(MGD)_2 + DAsc \quad (17a)$$

$$Asc\text{-}H \xleftrightarrow{K_a} Asc^- + H^+ \quad (17b)$$

where k_{red}, K_a or DAsc are the rate constant for the reduction reaction, the equilibrium constant or dehydroascorbate, respectively. The time change of optical absorption of the solution during the reaction is described as

$$D_t = \frac{D_{min} \cdot (D_0 - D_{min})}{\left\{1 + k_{red}[Asc^-]_0 \frac{[NO\text{-}Fe^{3+}(MGD)_2]_0 t}{(1+[H^+]/K_a)}\right\}} \quad (18)$$

where D_t is a total absorption of the solution in time $\{\varepsilon_1[NO\text{-}Fe^{3+}(MGD)_2] + \varepsilon_2[NO\text{-}Fe^{2+}(MGD)_2]\}$; $D_0 = \varepsilon_1[NO\text{-}Fe^{3+}(MGD)_2]_0$ (initial optical absorption of the complex); D_{min} is a final absorption of the solution caused with product of the reaction, $NO\text{-}Fe^{2+}(MGD)_2$. Linearization of the dependence 18 in $1/(D_t - D_{min})$ coordinate versus t observed experimentally (Fig.6, right panel) allows to estimate the value of k_{red} from the equation

$$k_{red} = tg\alpha \cdot \frac{1+[H^+]/K_a}{[Asc\text{-}][NO\text{-}Fe^{3+}(MGD)_2]_0}. \quad (19)$$